

Nutrient streams and their induction into the mixed layer

Richard G. Williams,¹ Vassil Roussenov,¹ and Michael J. Follows²

Received 15 July 2005; revised 9 November 2005; accepted 12 December 2005; published 22 March 2006.

[1] Nutrients are transferred from the nutricline into the winter mixed layer through a combination of vertical and lateral advection, referred to here as induction, the reverse of the subduction process. This advective supply of nutrients maintains the high productivity at high latitudes over timescales of several years and longer. Climatological diagnostics over the North Atlantic reveal that the induction of nutrients into the winter mixed layer is dominated by lateral advection even in the subpolar gyre where there is significant Ekman upwelling. The induction flux of nutrients is itself sustained by nutrient streams, strong nutrient transport associated with the western boundary currents. In the North Atlantic basin, the integrated induction flux accounts for typically 40% of the nitrate flux in the nutrient stream at 36°N, while the remaining fraction is recirculated in the thermocline of the subtropical gyre. The relationship between the nutrient stream and induction flux is illustrated using a numerical model of the circulation and biogeochemistry of the North Atlantic. The model studies suggest that the nutrient stream preferentially supplies nutrients to isopycnals outcropping in the subpolar gyre. The nutrient sources for the nutrient stream are either mode waters originating from the Southern Ocean or the tropics, where the eastern upwelling circulation and particle fallout focuses nutrients onto the lighter isopycnal surfaces of the nutrient stream.

Citation: Williams, R. G., V. Roussenov, and M. J. Follows (2006), Nutrient streams and their induction into the mixed layer, *Global Biogeochem. Cycles*, 20, GB1016, doi:10.1029/2005GB002586.

1. Introduction

[2] Basin-scale patterns of biological production are often explained in terms of vertical processes supplying nutrients to the euphotic zone. However, *Pelegri and Csanady* [1991] and *Pelegri et al.* [1996, 2006] have emphasized how boundary currents provide a crucial transport of nutrients within ocean basins which sustain the levels of biological production at high latitudes. They highlighted how the boundary currents lead to a “nutrient stream,” a region of a high nutrient flux, vN , where v is the velocity along the boundary current and N is the nutrient concentration. While the velocity of the boundary current is a maximum at the surface, the nutrient flux is often a maximum below the surface, since the surface concentrations of inorganic nutrients are often low or exhausted over the subtropical gyre (Figures 1a and 1b). In the North Atlantic, the nitrate flux associated with the Gulf Stream increases by a factor of 3 from Florida Strait (24°N) to 36°N, reaching 677 kmol s⁻¹ for waters lighter

than $\sigma = 27.5$ [*Pelegri et al.*, 1996]. Typically, half of this nitrate flux appears to pass into the subpolar gyre and half recirculates within the subtropical gyre.

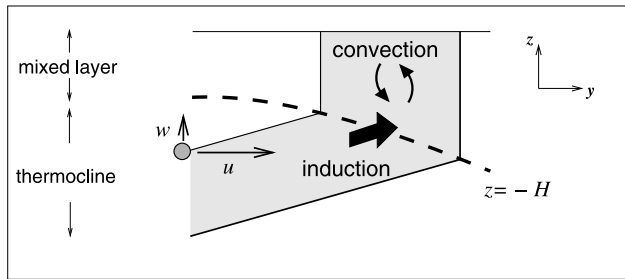
[3] In this study, we seek to complement the studies of *Pelegri and Csanady* by addressing the following questions: What is the mechanism by which nutrients carried in the stream are transferred downstream into the euphotic zone? What fraction of the nutrient stream flux is transferred into the sunlit surface waters? What is the upstream source of the nutrients in the stream?

[4] The mechanism by which the nutrients in the stream are transferred to the surface is explored through climatological subduction diagnostics. Here we focus on the flux of volume and nitrate passing into the seasonal boundary layer from the main thermocline, which we refer to as induction, the reverse of the subduction process [*Williams*, 2001] (section 2); note though that the rate of transfer from the main thermocline is also called the obduction rate by *Qiu and Huang* [1995]. The relationship of the induction process to the nutrient stream is investigated by comparing our induction diagnostics with those of *Pelegri et al.* [1996] for the nutrient stream integrated over the same density classes. The pathways of the nutrient stream in the North Atlantic and its connection to the induction process is addressed by using a coupled isopycnal circulation model and a simplified nitrate and dissolved organic nitrogen model (section 3). The formation and downstream fate of the nutrient stream is examined using idealized tracer experiments together

¹Department of Earth and Ocean Sciences, University of Liverpool, Liverpool, UK.

²Program in Atmospheres, Oceans and Climate, Department of Earth Atmosphere and Planetary Sciences, Massachusetts Institute of Technology, Cambridge, Massachusetts, USA.

a) transfer of fluid from the thermocline to the mixed layer



b) nutrient stream and its downstream transfer

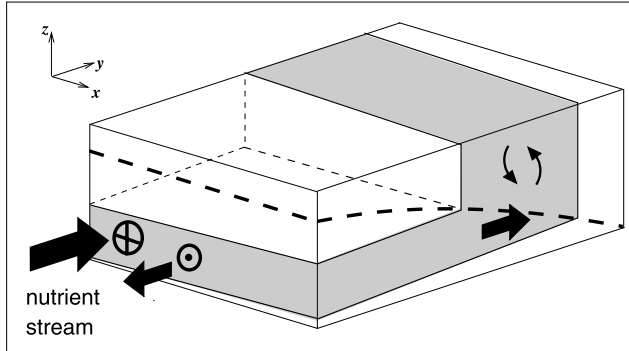


Figure 2. A schematic figure depicting the induction process where fluid and nutrients are transferred from the thermocline into the mixed layer: (a) a meridional section where a particle moves with a vertical velocity, w , and a horizontal velocity, u , leading to a vertical and lateral transfer into a poleward thickening mixed layer; (b) a three-dimensional view where a nutrient stream associated with the western boundary current transfers nutrients into the downstream mixed layer, which are then vertically redistributed through convection. The shading denotes an isopycnal layer and the dashed line the base of the mixed layer.

with diagnostics of observed nutrient and tracer distributions (section 4). Finally, there is a discussion of how the nutrient pathways and induction process regulate the gyre and basin-scale patterns of productivity over the Atlantic (section 5).

2. Nutrient Streams and the Induction Process

[5] The nutrient stream only influences the export production when its flux of nutrients is transferred to the euphotic zone. Given that the nutrient stream is a subsurface feature at 36°N , this downstream supply of nutrients involves a two stage process (Figure 2a). First, the nutrients have to be transferred from the nutrient stream into the winter mixed layer, through the reverse of the subduction process (referred here to as “induction”), and second, the nutrients have to be transferred within the seasonal boundary layer via convection to the euphotic zone. In our view, the rate limiting process determining the annual supply of nutrients to the euphotic zone is the induction process, the transfer of nutrients into the winter mixed layer and sea-

sonal boundary layer, while the subsequent seasonal cycle of the mixed layer and convection dictates the timing of any peaks in productivity, such as the spring or autumn blooms.

2.1. Climatological View of the End of Winter Conditions

[6] The instantaneous mixed layer distribution is highly variable in time through the diurnal and seasonal cycles in surface forcing, and the passage of synoptic-scale weather systems, as well as highly variable in space through stratification changes linked with ocean mesoscale eddy and frontal features. In order to provide a large-scale context for the nutrient transfer process, it is useful to define an interface marking the maximum extent of the convection process, or the seasonal boundary layer, given by the thickness of the mixed layer at the end of winter, H . This interface is diagnosed over the North Atlantic from climatological density profiles, defined by the depth where the potential density has increased by 0.125 kg m^{-3} from the surface density. The end of winter mixed layer is characterized by a thickness of 50 m over the tropics, increasing poleward to 200 m over the northern flank of the subtropical gyre, then increasing to more than 300 m following a cyclonic circuit of the subpolar gyre (Figures 3a and 3d). Concomitant with the poleward thickening of the mixed layer, there is an increase in the mixed-layer density from less than $\sigma_\theta = 24.0$ in the tropics, reaching $\sigma_\theta = 26.75$ and 27.0 over the subtropical/subpolar boundary and increasing further to $\sigma_\theta = 27.5$ in the northwest corner of the subpolar gyre (Figure 3b). This poleward thickening of the mixed layer is also associated with an increase in the nitrate concentration for the end of winter mixed layer, N_H , which ranges from less than 1 to $5 \mu\text{M}$ over the subtropical gyre and increases from 5 to $15 \mu\text{M}$ ($\text{M} \equiv \text{mol L}^{-1}$) over the subpolar gyre (Figure 3c); N_H is taken from the nitrate value at the depth H interpolating from the climatological nitrate profile [Conkright *et al.*, 1994; Glover and Brewer, 1988].

[7] Convection is important in vertically redistributing nutrients within the mixed layer and seasonal thermocline on seasonal and interannual timescales and thus provides a nutrient flux into the euphotic zone [Williams *et al.*, 2000]. However, if there is an export flux through the base of the winter mixed layer, then convection cannot sustain the nutrient concentrations within the seasonal boundary layer over several annual cycles, as the convective flux by definition goes to zero at the base of the winter mixed layer [Williams and Follows, 1998]. There has to be another mechanism to resupply the nutrients within the seasonal boundary layer. While traditionally, this resupply has been invoked in terms of a vertical diffusion or vertical advection, instead we advocate the isopycnic transport of nutrients [Williams and Follows, 2003].

2.2. Annual Rate of Subduction and Induction Over the North Atlantic

[8] The most important process in sustaining the end of winter nutrient concentrations in the mixed layer over a basin is the background gyre circulation, which involves both a vertical and horizontal transfer between the main thermocline and the end of winter mixed layer. The

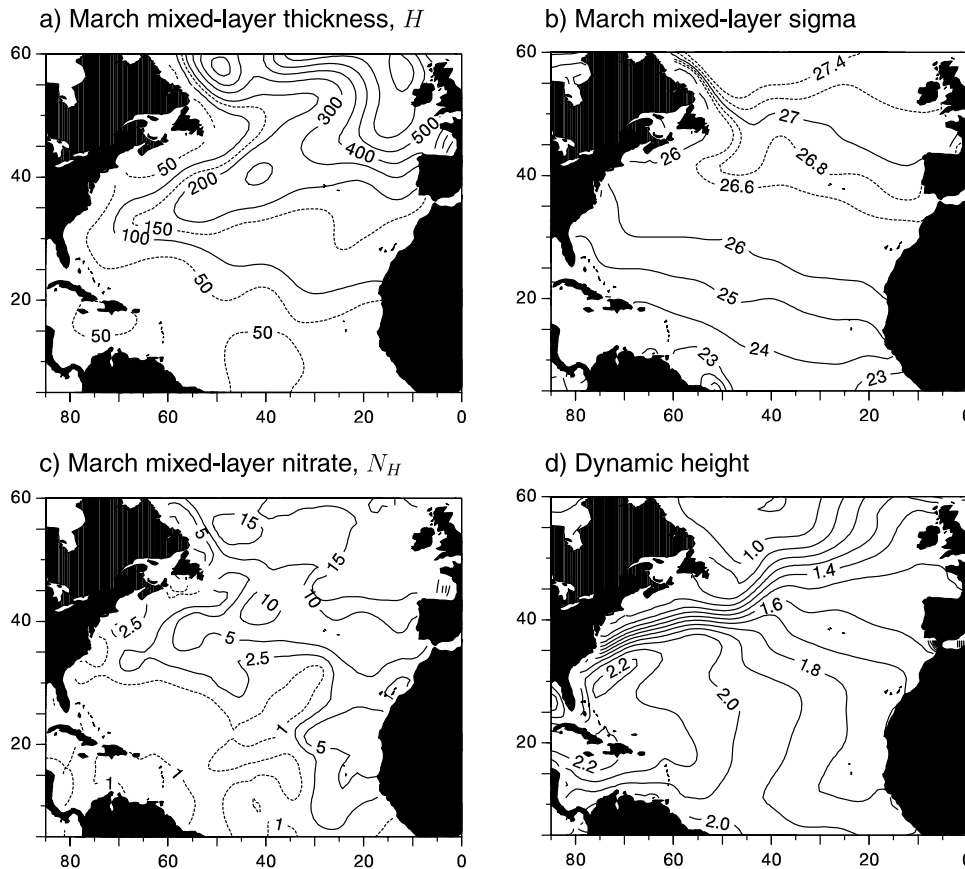


Figure 3. Climatological diagnostics of the mixed layer and circulation: (a) March mixed-layer thickness, H (m), from the *Levitus* [1982] climatology (smoothed to remove fine scales); (b) March mixed-layer σ_t with dashed contours covering the σ range of the nutrient stream; (c) March mixed-layer nitrate concentration, taken to be the same as the value at the top of the main thermocline, N_H (μM), diagnosed using climatological nitrate from *Conkright et al.* [1994]; (d) dynamic height field (m) at the surface relative to 2500 m derived by integrating the thermal-wind equations with the *Levitus* climatology.

volume flux transferred from the seasonal boundary layer into the main thermocline is defined by the subduction rate (Figure 2a) [Marshall *et al.*, 1993], which for climatological diagnostics can be evaluated as

$$S_{ann} = -w_H - \mathbf{u}_H \cdot \nabla H, \quad (1)$$

where H defines the interface given by the end of winter mixed layer and the top of the main thermocline, w and \mathbf{u} are the vertical velocity and horizontal velocity respectively at this interface. S_{ann} has units of m yr^{-1} , but should be viewed as a volume flux per unit area, $\text{m}^3 \text{yr}^{-1}/\text{m}^2$.

[9] The annual subduction rate is evaluated following *Marshall et al.* [1993], where full details are given. The horizontal velocity, \mathbf{u}_H , is evaluated assuming thermal-wind balance using the horizontal density gradients evaluated from the *Levitus* [1982] climatology assuming a level of no motion at 2.5 km or the seafloor if shallower (Figure 3d). The horizontal volume flux directed across the end of winter interface is evaluated from the scalar product, $\mathbf{u}_H \cdot \nabla H$.

[10] The vertical velocity at the base of the Ekman layer, w_{ek} , is diagnosed from the annually averaged surface winds

from the *Isemer and Hasse* [1987] climatology (Figure 4a), then the vertical velocity at the interface $z = -H$ is evaluated using linear vorticity balance

$$w_H = w_{ek} - \frac{\beta}{f} \int_{z=-H}^{z=0} v dz, \quad (2)$$

where f is the planetary vorticity, $\beta = df/dy$, and v is the meridional velocity.

[11] Our focus is on the volume and nitrate fluxes into the winter mixed layer, so we concentrate on the reverse of the subduction rate, $-S_{ann}$ (Figure 4b) [Williams, 2001]. The climatological diagnostics reveal that the volume flux into the winter mixed layer is greater than 300 m yr^{-1} over the Gulf Stream extension and over much of the subpolar gyre. In contrast, over much of the subtropical gyre, the volume flux is directed from the mixed layer into the main thermocline with S_{ann} reaching 100 m yr^{-1} over the gyre recirculation, but elsewhere is more typically 50 m yr^{-1} .

[12] The intensity of the subduction rate is much greater than the vertical wind-induced Ekman transfer, which only reaches a maximum magnitude of 50 m yr^{-1} , particularly

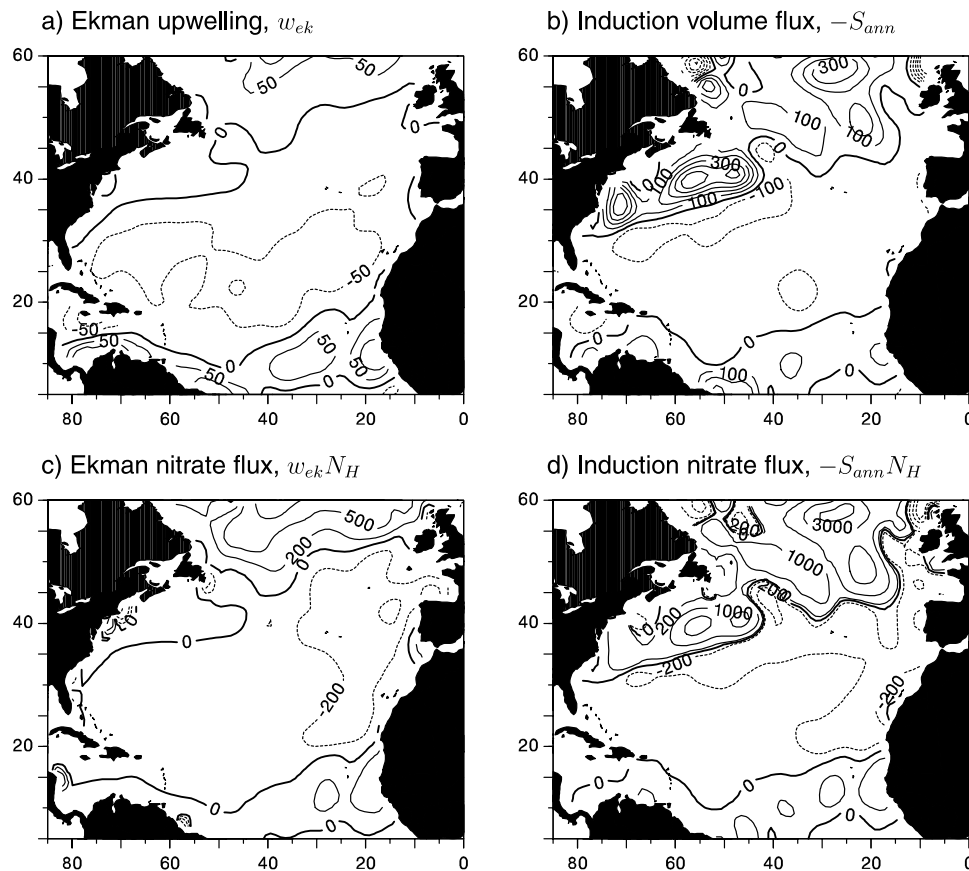


Figure 4. Climatological diagnostics of annual mean volume and nitrate fluxes in the upper ocean per unit horizontal area: (a) Ekman upwelling, w_{ek} and (b) volume flux from the thermocline into the base of the winter mixed layer, $-S_{ann}$ (m yr^{-1}), referred to here as an induction flux; (c) Ekman upwelling of nitrate, $w_{ek}N_H$, and (d) induction nitrate flux, $-S_{ann}N_H$ ($\text{m yr}^{-1}\mu\text{M}$). Positive represents a flux directed from the thermocline into the mixed layer.

over the Gulf Stream extension and recirculation, and over the subpolar gyre. In addition, the zero line of S_{ann} is much farther south than that of w_{ek} owing to the contribution from the lateral transfer between the mixed layer and the thermocline. A recent eddy-resolving model study of the subduction process is broadly supportive of these end of winter climatological diagnostics [Valdivieso da Costa *et al.*, 2005], although they highlight how the stronger flows in the Gulf Stream lead to enhanced subduction rates there.

2.3. Induction Flux of Nutrients Into the Winter Mixed Layer

[13] The induction flux of nutrients into the winter mixed layer is given by the product of the volume flux per unit area into the end of winter mixed layer, $-S_{ann}$, and the nutrient concentration at the top of the main thermocline (or equivalently at the base of the mixed layer at the end of winter), N_H ,

$$-S_{ann}N_H. \quad (3)$$

This induction flux of nutrients has the same units as used for the nutrient stream, the product of a velocity and a nutrient concentration. Choosing N_H to be nitrate now, there is a high

induction flux of nitrate into the mixed layer reaching more than $1000 \text{ m yr}^{-1}\mu\text{M}$ over the Gulf Stream extension and over the subpolar gyre (Figure 4d), which is to be expected given the patterns of N_H and $-S_{ann}$ (Figures 3c and 4b). Again this induction flux is much larger than the corresponding Ekman upwelling, $w_{ek}N_H$, which only reaches $500 \text{ m yr}^{-1}\mu\text{M}$ over the northern flank of the subpolar gyre (Figure 4c).

[14] While the Ekman upwelling induced by the winds ultimately controls the deformation of the thermocline and gyre circulation, this upwelling does not directly provide the dominant supply of nitrate to the mixed layer or euphotic zone. Instead the nutrient concentrations in the end of winter mixed layer on the basin scale are sustained by the induction of nutrients from the gyre circulation.

[15] The induction flux of volume and nutrients can be further separated into the contributions from the vertical and horizontal transfer into the end of winter mixed layer (Figure 5). The vertical transfer at the base of the winter mixed layer only makes a significant contribution to the induction flux in the tropics and on the northern flank of the subpolar gyre for both volume and nitrate (Figures 5a and 5c). In comparison, the horizontal contribution leads to large contributions to the induction fluxes of volume and nitrate along the Gulf Stream and over much of the subpolar

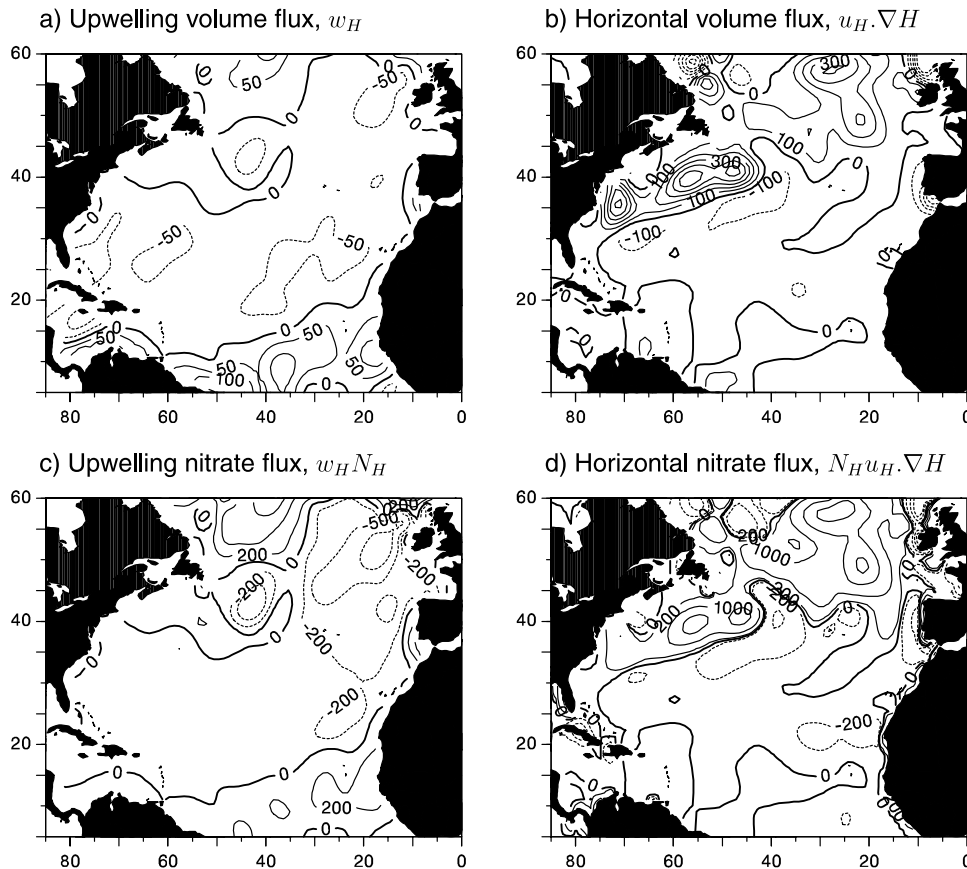


Figure 5. Climatological diagnostics of the vertical and horizontal components of the induction volume and nitrate fluxes per unit horizontal area: (a) vertical, w_H , and (b) horizontal volume flux, $u_H \cdot \nabla H$ (m yr^{-1}); (c) vertical nitrate, $w_H N_H$, and (d) horizontal nitrate flux, $N_H u_H \cdot \nabla H$ ($\text{m yr}^{-1} \mu\text{M}$). Positive represents a flux directed from the thermocline into the mixed layer.

gyre (Figures 5b and 5d). Thus the induction flux of volume and nitrate is sustained by the lateral, rather than vertical transfers into the winter mixed layer. These essential points hold even though the details of our diagnostics are sensitive to the choice of the climatological winds, background circulation and end of winter mixed-layer distribution.

2.4. Induction Flux of Nutrients and the Nutrient Stream

[16] In our view, the induction flux of the nutrients is itself sustained by the nutrient stream, although a significant fraction of the nutrient stream is not transferred into the mixed layer and instead recirculates within the subtropical thermocline (Figure 2b). Hence we expect that the nutrient flux in the stream to be comparable to the downstream induction into the seasonal boundary layer,

$$\int_{-D_o}^0 \int_{x_1}^{x_2} v N dx dz \sim \int_A (-S_{ann} N_H) dx dy, \quad (4)$$

where the left-hand integral is applied over the width of the boundary current from longitudes x_1 to x_2 and over the depth of isopycnals, D_o , that outcrop downstream within the basin, while the right-hand integral is applied over the horizontal area over which the density layers in the nutrient

stream outcrop. The terms in (4) are only expected to be comparable, rather than exactly balance. The advection in the nutrient stream is generally expected to be larger than the downstream induction owing to part of the nutrient stream recirculating and not contributing to the downstream transfer. Conversely, remineralization of biological fallout can lead to the nutrients increasing in concentration with time along the isopycnal layers, which might lead to the induction flux of nutrients sometimes exceeding the upstream advective flux within a particular density layer.

[17] Given this advective balance, it is useful to reexamine the mixed-layer winter distribution and nutrient stream diagnostics. The dominant part of the nutrient stream lies within a σ range of 26.6 to 27.4 (Figure 1c), which outcrops into the winter mixed layer over the northern part of the subtropical gyre and much of the subpolar gyre (Figure 3b, dashed contours). For the same outcrop region, there are elevated nitrate concentrations (Figure 3c). Hence the density class of the nutrient stream is broadly in accord with the downstream nutrient distribution in the winter mixed layer.

[18] To test this connection further, the subduction and induction fluxes of volume and nitrate are now separately diagnosed within σ classes over the North Atlantic south of 60°N (Table 1). The subduction contributions are summed only when $S_{ann} > 0$ and, conversely, the induction contribu-

Table 1. Diagnostics of Volume (Sv) and Nitrate (kmol s⁻¹) Area-Integrated Fluxes in Different Density Classes for Subduction and Induction Regions Over the North Atlantic, as Well as Nutrient Stream Diagnostics at 36°N by *Pelegri et al.* [1996]^a

σ Range	Nutrient Stream by <i>Pelegri et al.</i> [1996]		Subduction ($S_{ann} > 0$)		Induction ($S_{ann} < 0$)	
	$\int v dx dz$, Sv	$\int v N dx dz$, kmol s ⁻¹	$\int S_{ann} dA$, Sv	$\int S_{ann} N_H dA$, kmol s ⁻¹	$\int -S_{ann} dA$, Sv	$\int -S_{ann} N_H dA$, kmol s ⁻¹
25.6 ≤ σ < 26.2	6.6	44	9.2	24	6.0	13
26.2 ≤ σ < 26.5	8.0	59	7.3	22	5.0	23
26.5 ≤ σ < 26.8	12.5	155	4.2	29	5.7	31
26.8 ≤ σ < 27.1	11.7	219	1.9	18	8.2	89
27.1 ≤ σ < 27.3	5.0	113	2.3	22	4.5	68
27.3 ≤ σ < 27.5	3.6	87	1.7	18	4.0	60
Totals						
26.5 ≤ σ < 27.3	29.2	487	8.4	69	18.4	188
25.6 ≤ σ < 27.5	47.4	677	26.6	133	33.4	284

^aThe subduction and induction estimates are based on diagnostics from 5°N to 60°N over the Atlantic.

tions are only summed when $S_{ann} < 0$ for each density class; the density classes are chosen to be the same as those reported by *Pelegri et al.* [1996]. First, there is a relatively small subduction flux of volume and nitrate over the North Atlantic within the core of the nutrient stream, as defined by the σ range from 26.5 to 27.3, reaching 8.4 Sv and 69 kmol s⁻¹ (Table 1). This subduction process leads to the relatively depleted nutricline over the subtropical gyre, as discussed in terms of 18C mode water by *Palter et al.* [2005].

[19] Second, within the same σ range of 26.5 to 27.3, there is a much larger induction flux of volume and nitrate associated with the nutrient stream reaching 18.4 Sv and 188 kmol s⁻¹ (Table 1). In comparison, *Pelegri et al.* [1996] diagnose a maximum volume flux of 29.2 Sv and an associated nitrate flux of 487 kmol s⁻¹ within these same density classes passing through a section crossing the Gulf Stream at 36°N. Thus our diagnostics suggest that typically 40% of the nutrient stream sustains the downstream induction process.

[20] In our view, the principle differences between the induction and nutrient stream estimates of the volume and nitrate fluxes are due to recirculating components being included in the nutrient stream diagnostics of *Pelegri et al.* [1996]. In addition, our diagnostics of the induction process are based upon climatological diagnostics, which probably underestimate the circulation and volume flux. While our induction fluxes are smaller than that diagnosed by *Pelegri et al.* [1996], there is a broadly similar σ distribution with the maximum flux concentrated in the band from 26.8 ≤ σ < 27.1. Our later model diagnostics show larger induction fluxes of nitrate, as well as a larger fraction of the nutrient stream being inducted into the downstream mixed layer (between 63% and 82% varying with the σ range; see Table 2 in section 3.4). In order to explore the connection between the nutrient stream and downstream induction process in a more dynamically consistent manner, we now examine the nutrient pathways within an isopycnal circulation model.

3. A Model Study of the Downstream Effect of the Nutrient Stream

3.1. Model Formulation

[21] The model study employs an isopycnal model (MICOM 2.7 [Bleck and Smith, 1990]) with a formulation

similar to that employed by *Roussenov et al.* [2004]. The model includes 15 isopycnal layers in the vertical plus a surface mixed layer with variable density and a horizontal resolution of 1.4° on a Mercator grid (150 km at the equator and 75 km at 60°N). The model topography is based on ETOP05 data averaged within the model grid. There is a diapycnic diffusivity, $\kappa = 10^{-7}/N$, varying with buoyancy frequency N , which typically varies from 10⁻⁵ m² s⁻¹ in the thermocline to 10⁻⁴ m² s⁻¹ in the deep waters. In addition, the isopycnal model employs isopycnal mixing and thickness diffusion (using a diffusive velocity of 0.5 cm s⁻¹ with Laplacian and biharmonic forms, respectively), and deformation-dependent momentum mixing (using a mixing velocity of 1 cm s⁻¹ with a background Laplacian dependence).

[22] The model is forced using monthly wind stress, surface freshwater fluxes, surface radiative fluxes, with latent and sensible heat fluxes calculated from air temperature and water vapor mixing ratio from ECMWF (ERA20). Rivers are added as freshwater fluxes at corresponding coastal grid points. The Strait of Gibraltar is closed, but the salinity of subsurface layers at this location is relaxed to climatology on a 30-day relaxation timescale. On the northern and southern boundaries, there is a “sponge relaxation” to climatology (with a relaxation timescale increasing from 30 to 180 days) for temperature in the mixed layer, salinity and the height of density interfaces for all layers. The model is initialized from *Levitus* [1982] climatology (temperature, salinity and density) and integrated for an initial spin-up of 60 years and then for a further 40 years in an online coupled mode for nutrient and tracer experiments.

3.2. Nutrient Cycling

[23] The total nitrogen is separated into nitrate, dissolved organic nitrogen (DON) consisting of semilabile and refractory components, and particulate organic nitrogen (PON). The PON is assumed to fallout and be remineralized in the interior with a vertical scale of 200 m, while the dissolved inorganic, semilabile and refractory organic nutrients are assumed to be transported by the circulation with lifetimes in the euphotic zone of typically 6 months and 6–12 years, respectively; see further details in Appendix A.

[24] The initial nitrate is taken from climatology [Conkright et al., 1994] while the semilabile DON is initialized to be 0 and the refractory DON initialized as

2 μM below 2 km and 4 μM above 2 km. On the open boundaries, nitrate is continuously relaxed to the initial condition within the buffer zones, and there are no atmospheric or riverine inputs of nutrients, or any loss of nutrients on the seafloor through burial. The nitrogen model is integrated for 40 years online after the 60-year dynamical spin-up.

[25] The model broadly captures the observed meridional structure of the nitrate distribution (Figure 6a). There is a plume of high nitrate associated with the sub-Antarctic mode water and Antarctic Intermediate Water, passing into the domain from 20°S at depths from 500 m to 1500 m. In the data, the plume becomes diluted northward of 20°N and eventually is not a distinct feature at higher latitudes. In the model, there is a similar dilution of the plume, but this weakening starts north of the equator. In deep waters below 500 m, the lowest nitrate concentrations are in the subpolar gyre, reflecting the relatively recent ventilation and low age there.

[26] For maps of the annually averaged, surface nitrate in the model and the climatological data, there is the expected northward increase in nitrate concentrations associated with the thickening of the winter mixed layer over the North Atlantic (Figure 6b). The model overestimates the surface nitrate by 1 to 3 μM over the subtropics of the North Atlantic, which might be owing to a convergence of nutrient-rich intermediate waters from the southern ocean (which should instead be advected farther north). At the same time, the model underestimates the surface nitrate by up to 5 μM in the upwelling zones centered off Africa at 15°N and 20°S, which might be owing to the upwelling being too weak through only using monthly averaged wind forcing.

[27] The modeled DON over the euphotic zone has elevated concentrations in the tropics (10°S–5°N) with lower values at 20°S and 40°N (Figure 6c). The modeled PON export ranges from 0.05 $\text{M m}^{-2} \text{yr}^{-1}$ over much of the tropical and subtropical Atlantic and increasing to 0.35 $\text{M m}^{-2} \text{yr}^{-1}$ over higher latitudes and the African upwelling zones centered at 20°N and 20°S (Figure 6d). This pattern is broadly in accord with the adjoint model estimates of export production by *Usbeck et al.* [2003] where the model is constrained by nitrate observations and, to a lesser extent, sediment trap observations.

3.3. Model Trajectories and the Nutrient Stream

[28] The nutrient model is now used to consider how the nutrient stream is formed and its downstream effect. For reference, the depth-integrated transport has the classical anticyclonic circulation over the subtropical gyre (10°N to 40°N–50°N) and cyclonic circulation over the subpolar gyre. The depth-integrated horizontal transport reaches 35 Sv (1 Sv = $10^6 \text{ m}^3 \text{ s}^{-1}$) over the Gulf Stream, which is consistent with the wind stress curl forcing. Owing to the relatively coarse horizontal resolution, the model does not capture the observed downstream strengthening of the boundary current from 94 Sv at 73°W to 149 Sv at 55°W [Hogg, 1992].

[29] In order to understand the pathway of the nutrient stream, Lagrangian trajectories are calculated along the $\sigma = 27.03$ surface. The float trajectories are advected by the

monthly mean velocity along the $\sigma = 27.03$ surface or by the mixed-layer velocity when the σ surface has outcropped. The trajectories are either (1) released at every second model grid point over the entire domain and integrated for 3 years (Figure 7a) or (2) only released at every second grid point along 20°S and integrated for 50 years (Figure 7b). First, trajectories leaving the Gulf Stream spread into both the subtropical and subpolar gyres (Figure 7a) and thus provide a nutrient flux into both gyres, as argued by *Pelegri and Csanady* [1991]. Trajectories remaining within the subtropical gyre eventually rejoin the Gulf Stream and can provide an additional nutrient flux to the boundary current. There are also recirculating trajectories within the subpolar gyre which circuit the northern North Atlantic through the cyclonic interior gyre circulation and the southward Labrador Current. Second, trajectories associated with the influx of nutrients in the Gulf Stream partly originate from south of the equator along the western boundary (Figure 7b). All of these trajectories become more complex and include more recirculating components as the model resolution increases. This Lagrangian view is taken further in subsequent tracer release experiments.

[30] In the model, the nitrate stream is revealed by a subsurface region of high nitrate flux running northward from the southern boundary along the western boundary, crossing the equator, and continuing to 36°N where the nitrate stream leaves the western boundary and crosses to the eastern side of the subpolar gyre (Figure 7b, shaded). The core of the nutrient stream is along $\sigma = 27.03$, where a nitrate tongue extends northward from the tropics through the western boundary advection (Figure 7b, dashed contours).

[31] In the model, the meridional overturning reaches 19 Sv (as given by the northward transport over the upper 1500 m) and leads to a northward zonally integrated nitrate flux with a southern maximum of typically 300 kmol s^{-1} (Figure 7c, solid and short-dashed lines). However, the nitrate flux integrated across the nutrient stream is much larger, reaching nearly 900 kmol s^{-1} , thus revealing that much of the nutrient stream is recirculated (Figure 7c, long-dashed lines). This model solution differs though from the inverse analysis of *Rintoul and Wunsch* [1991], who diagnosed a northward zonally integrated nitrate transport of $119 \pm 35 \text{ kmol s}^{-1}$ at 36°N and $-8 \pm 39 \text{ kmol s}^{-1}$ at 24°N. This difference probably reflects an underestimate of the gyre circulation from the numerical model.

[32] Along 36°N, the model velocity section reaches 35 cm s^{-1} and there is an associated high nitrate flux centered at a depth of 500 m (Figure 8a). In density space, the modeled nitrate stream has two maxima reaching 4 $\text{mM m}^{-2} \text{ s}^{-1}$, located between $\sigma = 26.9$ to 27.3 (Figure 8b). In comparison, the diagnostics of *Pelegri and Csanady* [1991] along 36°N reveal a higher nitrate flux of greater than 10 $\text{mM m}^{-2} \text{ s}^{-1}$ at slightly shallower depths from 250 m to 750 m and within a σ range of 26.7 to 27.2 (Figures 1b and 1c). Associated with the nitrate stream, there is also a high DON flux reaching 2.5 $\text{mM m}^{-2} \text{ s}^{-1}$ concentrated within the upper 500 m and in the lighter range of $\sigma = 26.4$ to 26.7. The DON stream transfers high concentrations of DON in the tropics to higher latitudes within the North Atlantic (Figure 6c). This signal is smaller than the

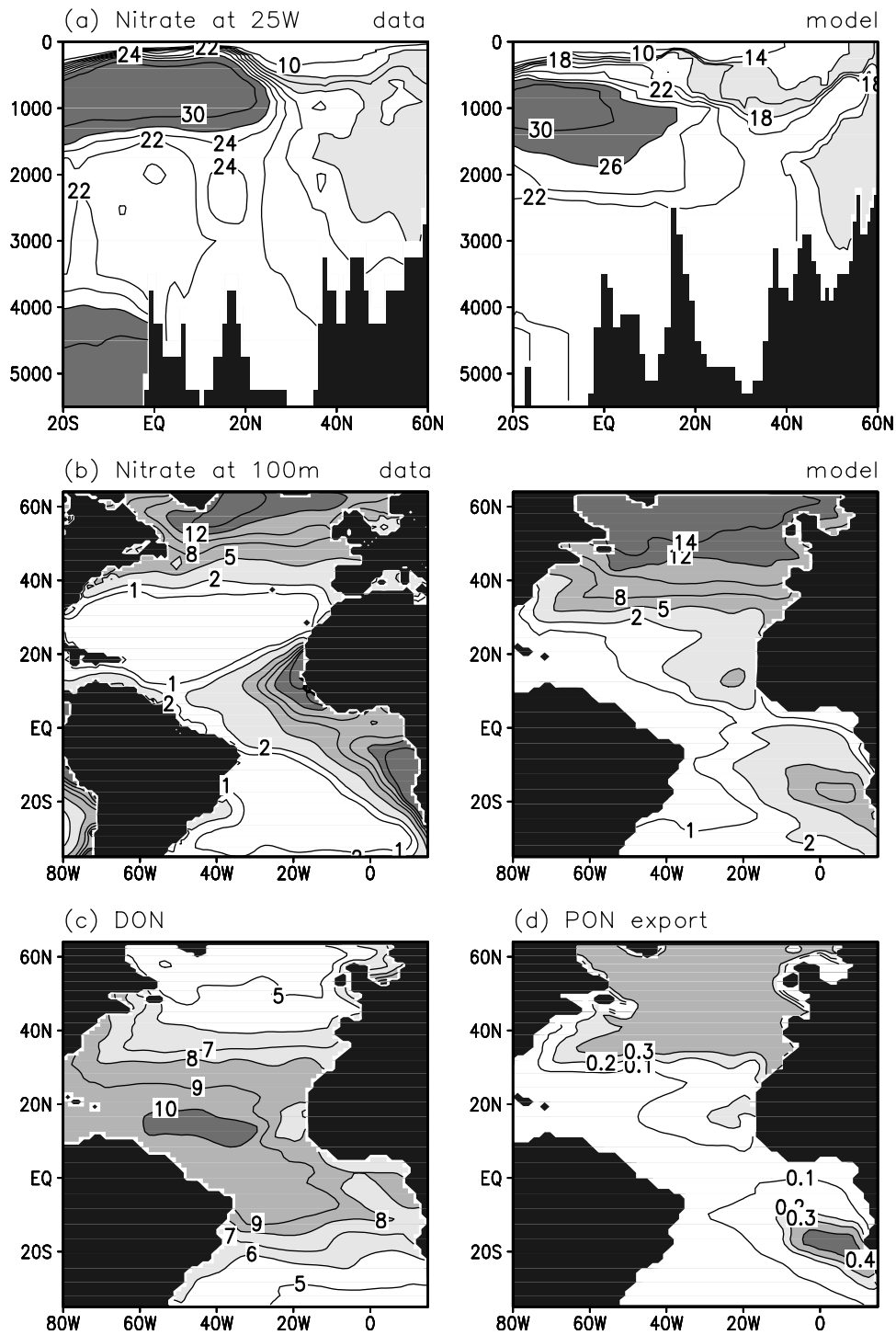


Figure 6. Nitrate distributions (μM) from (left) climatology and (right) the model for (a) meridional section along 25°W and (b) maps of nitrate concentration averaged over the upper 100 m, together with model maps for (c) concentrations of DON (μN) in the upper 100 m and (d) annual export of particulate organic nitrogen (PON) at a depth of 100 m ($\text{M m}^{-2} \text{yr}^{-1}$).

modeled nitrate flux by a factor of 2, but still represents a potentially important nutrient pathway within the North Atlantic [Rintoul and Wunsch, 1991; Mahaffey et al., 2004].

[33] The modeled nutrient stream is also revealed at 20S by a high nitrate flux along the western boundary, which

stays confined to the western boundary to the equator (Figure 8c). The nutrient stream strengthens in intensity across the equator and reaching a maximum at 36°N , reflecting the combination of the input of nutrient-rich thermocline waters and the strengthening of the boundary

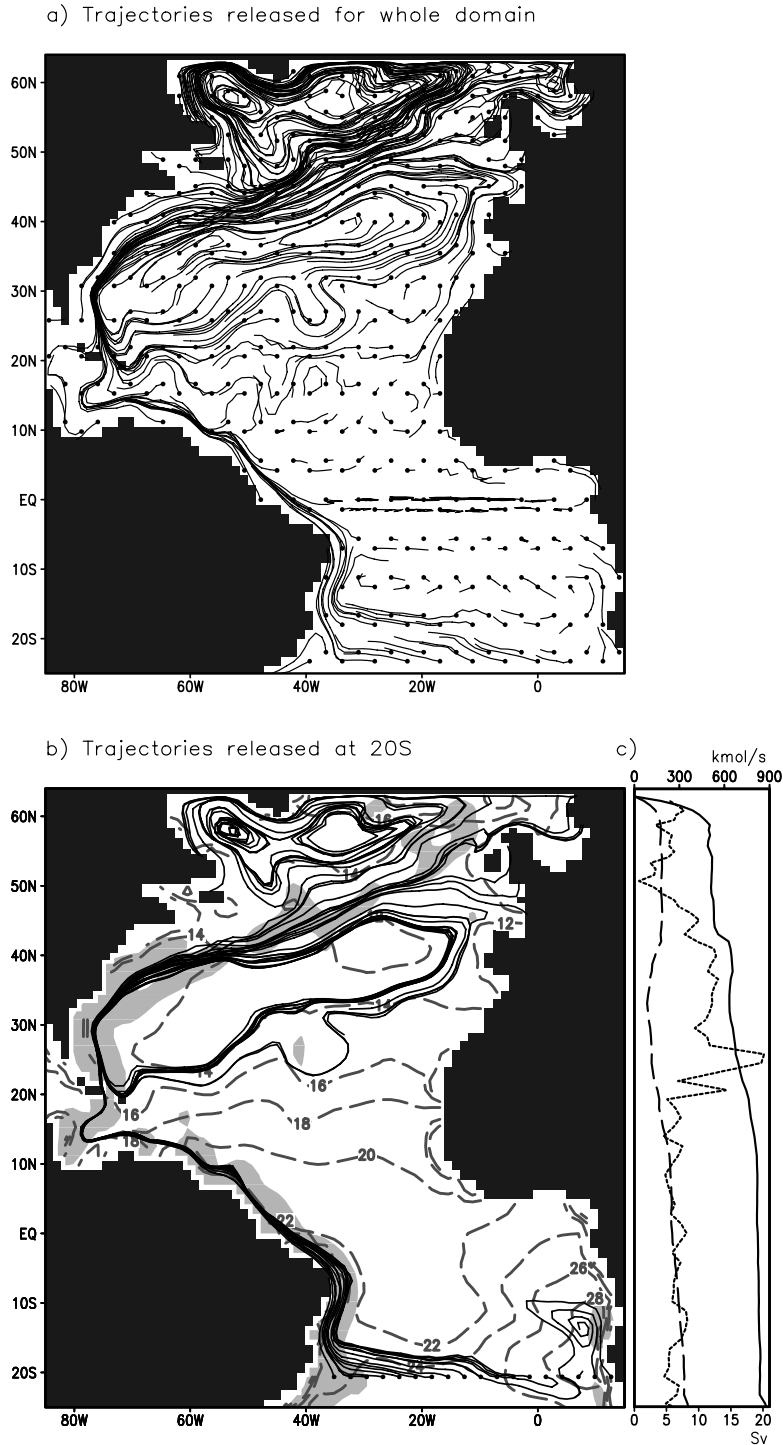


Figure 7. Model diagnostics of Lagrangian float trajectories along $\sigma = 27.03$ and for the mixed layer wherever the layer outcrops with dots representing the starting position. The floats are released at every second model grid point either (a) over the whole domain and integrated for 3 years or (b) only released along 20°S and integrated for 50 years. In Figure 7b, model nitrate in layer 27.03 (μN) is included (dashed contours) and the core of the nutrient stream is shaded, as defined by regions of high nitrate fluxes $>20 \text{ kmol s}^{-1}$ over the upper 1500 m. In addition, (c) zonally integrated diagnostics are included for the transport over the upper 1500 m (solid line, Sv), the nitrate flux (kmol s^{-1}) over the width of the basin (long-dashed line) and the core of the nutrient stream (short-dashed line).

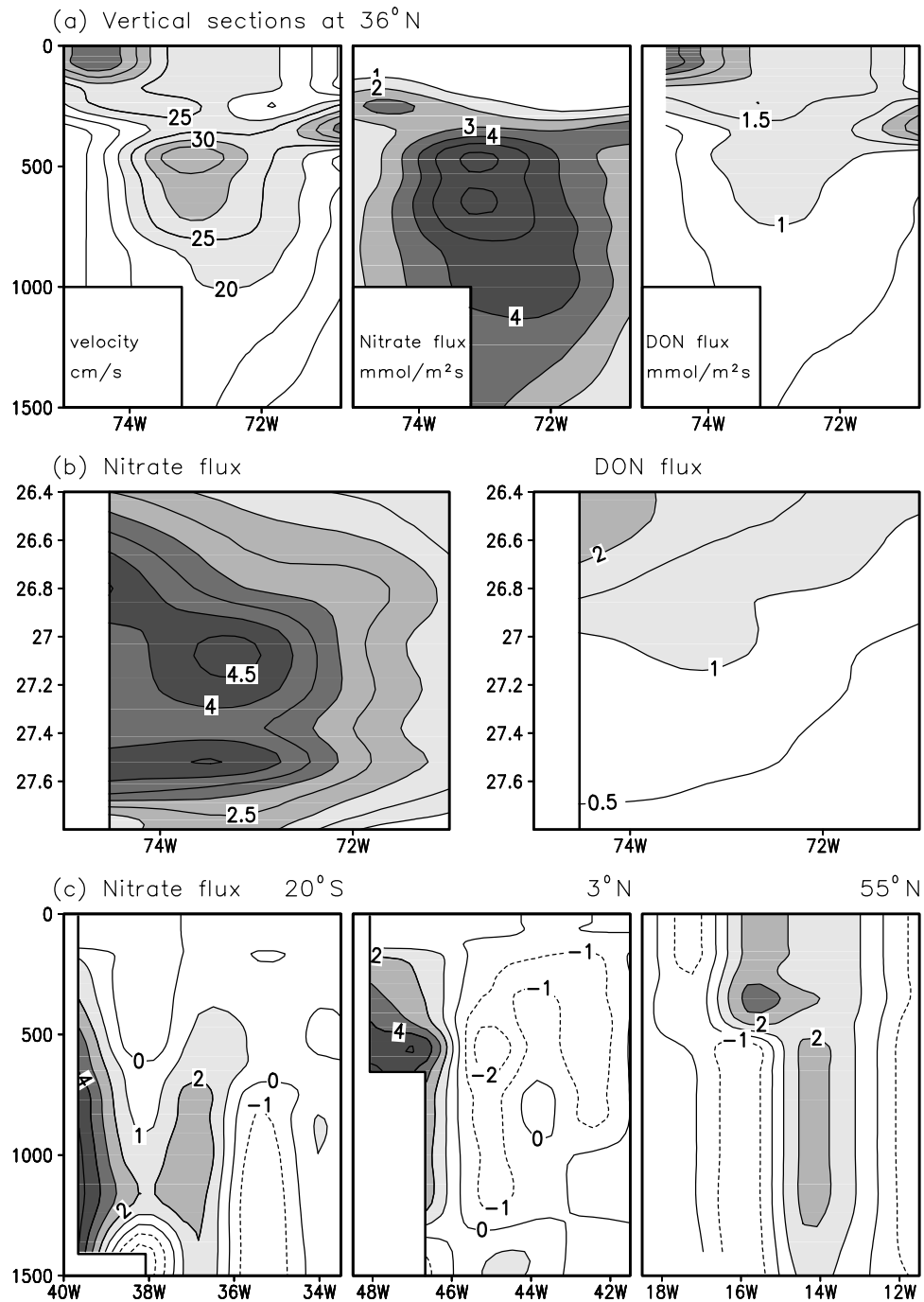


Figure 8. Modeled nutrient stream: (a) vertical sections at 36°N for the northward velocity (cm s^{-1}), nitrate and DON flux ($\text{mM m}^{-2} \text{s}^{-1}$) through the section; (b) σ sections at 36°N of nitrate and DON flux (with a smaller contour interval); and (c) depth sections of the nitrate flux at 20°S, 3°N and 55°N.

current, then weakens downstream (Figure 7c). The nutrient stream crosses the North Atlantic, eventually leading to northward flux on the eastern boundary of the subpolar gyre (Figure 8c).

3.4. Model Relationship Between the Nutrient Stream and Downstream Induction of Nutrients

[34] In the data-based diagnostics, we argued that the depth-integrated northward flux of nutrients in the Gulf

Stream sustains the area-integrated induction flux of nitrate into the downstream mixed layer (Table 1). These diagnostics are repeated for the model experiments for the transport of nitrate, as well as total nitrogen, the sum of nitrate and DON (Table 2). The diagnostics are reported for combined density bands within the model, broadly corresponding to those chosen by *Pelegri et al.* [1996].

[35] Over the broad western boundary region from the western coast to 70°W, the northward volume and nitrate

Table 2. Model Diagnostics of Volume (Sv) and Nitrate (kmol s^{-1}) Area-Integrated Fluxes in Different Density Classes^a

σ Range	Nutrient Stream		Subduction ($S_{\text{sum}} > 0$)		Induction ($S_{\text{sum}} < 0$)	
	$\int v \, dydz$, Sv	$\int v \, N \, dydz$, kmol s^{-1}	$\int S_{\text{sum}} \, dA$, Sv	$\int S_{\text{sum}} \, N_{\text{II}} \, dA$, kmol s^{-1}	$\int -S_{\text{sum}} \, dA$, Sv	$\int -S_{\text{sum}} \, N_{\text{II}} \, dA$, kmol s^{-1}
$25.5 \leq \sigma < 26.4$	7.4	23 (79)	1.5	5 (16)	5.3	17 (58)
$26.4 \leq \sigma < 26.7$	3.7	39 (66)	0.4	4 (6)	1.2	11 (19)
$26.7 \leq \sigma < 27.1$	11.7	171 (224)	4.1	47 (70)	6.9	82 (119)
$27.1 \leq \sigma < 27.3$	7.2	122 (148)	6.5	89 (119)	7.5	103 (138)
$27.3 \leq \sigma < 27.5$	4.7	93 (109)	5.0	73 (96)	8.6	143 (182)
Totals						
$26.4 \leq \sigma < 27.3$	22.6	332 (438)	11.0	140 (195)	15.6	196 (276)
$25.5 \leq \sigma < 27.5$	34.7	447 (626)	17.5	218 (307)	29.5	356 (516)

^aNutrient stream diagnostics from the meridional flux across 36°N (integrated from the western coast to 70°W) and separate subduction and induction diagnostics (integrated over the surface area from 5°N to 60°N). Estimates in brackets are for fluxes of total nitrogen, $\text{NO}_3 + \text{DON}$ (kmol s^{-1}).

fluxes are 22.6 Sv and 332 kmol s^{-1} in the σ range of 26.4 to 27.3, which are less than the 29.2 Sv and 487 kmol s^{-1} diagnosed by Pelegri *et al.* [1996]. In the same density range, the modeled subduction flux of volume and nitrate reaches 11.0 Sv and 140 kmol s^{-1} , which is larger than our data-based diagnostics of 8.4 Sv and 69 kmol s^{-1} . The modeled induction flux of volume and nitrate reaches 15.6 Sv and 196 kmol s^{-1} , which is broadly comparable to our data-based diagnostics of 18.4 Sv and 188 kmol s^{-1} . Thus, in the model, typically 63% of the northward nitrate flux associated with the nutrient stream (332 kmol s^{-1} , evaluated between the western boundary and 70°W) is inducted into the downstream mixed layer (196 kmol s^{-1}). In the data diagnostics, the comparable proportion is 40% suggesting that there is a weaker recirculating component included in the model.

[36] If these model diagnostics for the nitrogen flux are repeated to include the contribution of DON, then the northward depth-integrated nitrogen flux in the Gulf Stream increases from 332 kmol s^{-1} to 438 kmol s^{-1} within the σ range of 26.4 to 27.3, while the corresponding area-integrated induction flux increases from 196 kmol s^{-1} to 276 kmol s^{-1} (Table 2). Thus the transport of DON alters the total nitrogen supply (V. Roussenov *et al.*, Does the transport of dissolved organic nutrients affect export production in the Atlantic Ocean?, submitted to *Global Biogeochemical Cycles*, 2005). We now conduct tracer experiments to reveal how the nutrient stream is formed and its downstream effect.

4. How Is the Nutrient Stream Formed and What Is Its Fate?

4.1. Downstream Effect of the Nutrient Stream

[37] In order to understand the influence of the nutrient stream, tracer-release experiments are conducted, which are initialized with the model spin-up of 60 years and integrated online with the circulation model. First, a tracer is continuously released with a source value of 1 in the Gulf Stream along layer $\sigma = 26.52$, which is the lightest part of the nutrient stream; the source is applied along a zonal band, 1.4° wide along 36°N from the western coast to 65°W . Second, a twin experiment is conducted with the patch of tracer tracked for a further 20 years, but with the tracer source switched off. In the twin experiment, the tracer is either treated in (1) a conserved manner or (2) as a tracer

mimicking the cycling of nitrate. In this latter case, the tracer is consumed in the euphotic zone, then redistributed at depth through particle fallout and remineralization with a remineralization depth scale of 200 m (in accord with the nitrate model described in Appendix A, but without cycling of DON). In both tracer integrations, the same volume of tracer is released.

[38] First, for the conserved tracer, most of the tracer remains within the subtropical gyre, but tracer does spread within the mixed layer northward of the winter outcrop for the source layer over the subpolar gyre (Figure 9a, top panel). The tracer concentration is greatest within the upper thermocline of the subtropical gyre (Figure 9a, bottom panel). The tracer spreads into neighboring layers from the source layer ($\sigma = 26.52$) primarily through the tracer spreading into different density classes within the mixed layer and then being subducted into the thermocline.

[39] Second, for the nitrate-like tracer, the tracer becomes depleted over much of the source layer within the subtropical gyre, but acquires relatively high concentrations within denser layers within the underlying thermocline (Figure 9b). The nitrate tracer is transferred into these denser layers of the thermocline via the particle flux and remineralization. The induction process then transfers the tracer from these denser layers into the downstream mixed layer, hence leading to higher tracer concentrations within the mixed layer over the subpolar gyre. Thus the model experiments suggest that the nutrient stream leads to elevated nutrient concentrations in the surface mixed layer of the subpolar gyre, rather than the subtropical gyre.

4.2. Nutrient Source From the Tropics or the Southern Ocean?

[40] The nutrient stream, sustaining the induction process, is obviously related to the high velocities associated with the western boundary currents and their extensions into the gyre interior. However, the nutrient stream has a subsurface maximum that is dictated by the product of the nutrient and velocity profiles. We now consider where the nutrients associated with the nutrient stream originate from.

4.2.1. Data Diagnostics

[41] The transport pathways are now considered in terms of the PO_4^* tracer [Broecker and Peng, 1982],

$$\text{PO}_4^* = \text{PO}_4 + \text{O}_2/175, \quad (5)$$

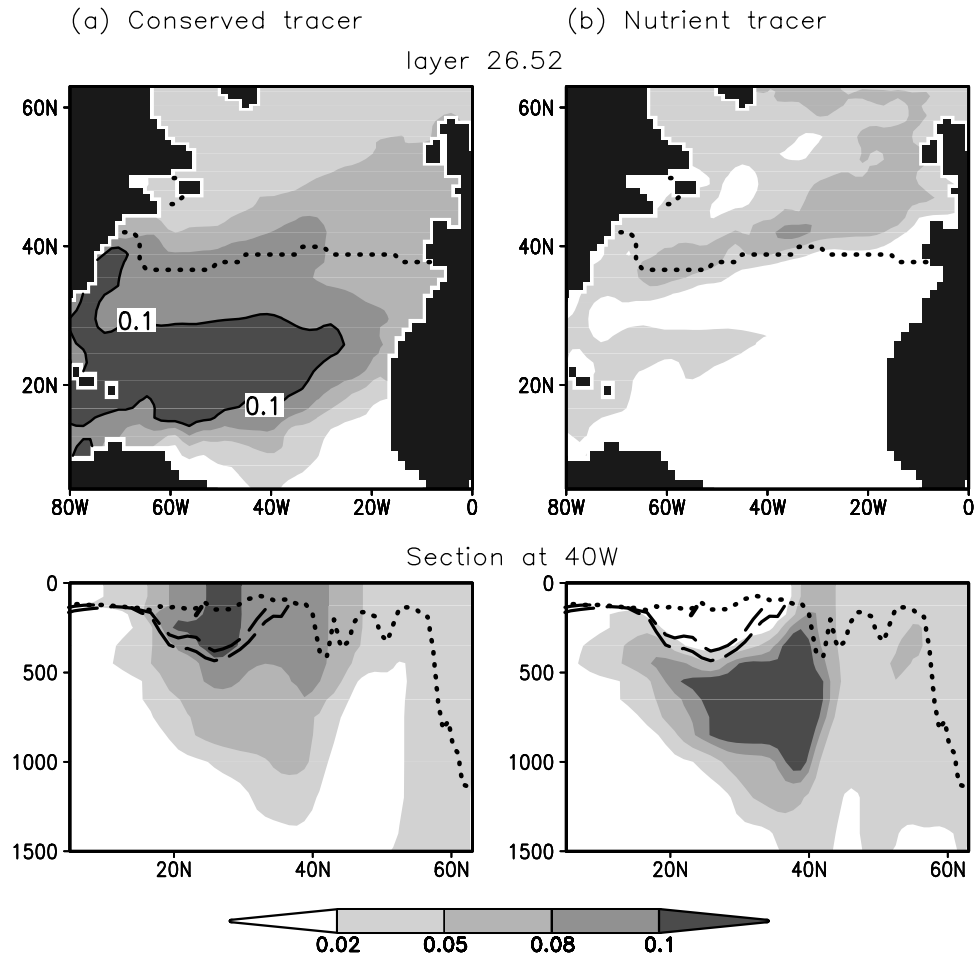


Figure 9. Twin experiments for tracer spreading from the Gulf Stream with the tracer either (a) conserved or (b) behaving like nitrate with consumption within the euphotic zone and remineralization at depth: (top) tracer concentrations (shaded) along the $\sigma = 26.52$ layer and the mixed layer with the end of winter outcrop (dotted line); (bottom) a vertical section along 40W with layer interfaces for $\sigma = 26.52$ (dashed line) and the base of the winter mixed layer (dotted line). Both tracer experiments are initialized with the same initial tracer distribution given by how a conserved tracer spreads for 20 years along $\sigma = 26.52$ with a continuous source of 1 in the Gulf Stream. The twin experiments are then integrated for a further 20 years without a source and with the tracer either (Figure 9a) conserved or (Figure 9b) behaving like nitrate. Note how the conserved tracer has higher concentrations in the subtropical gyre, but the nutrient tracer becomes more concentrated at depth and spreads mainly into the mixed layer over the subpolar gyre.

which is conserved for biotic reactions following Redfield stoichiometry, where the change in phosphate from remineralization of organic fallout is compensated by the oxygen consumed. Along the $\sigma = 26.5$, 27.0 and 27.5 surfaces making up the nutrient stream, the PO_4^* tracer reveals source waters with highest concentrations in the mode waters originating from the Southern Ocean (Figure 10, left panel). There is also a local maximum in the tracer concentration over the Labrador Sea in the northern subpolar gyre.

[42] The nitrate distributions are now considered along the same σ surfaces (Figure 10, right panel). Along the lighter surfaces, the highest nitrate concentrations are in the tropical upwelling zones off Africa centered at 15°S, reaching 25 μM and 35 μM along the $\sigma = 26.5$ and 27.0 surfaces,

respectively (Figures 10a and 10b) (see also D. Hansell and M. J. Follows, Nitrogen in the Atlantic Ocean, submitted to Nitrogen in the Marine Environment, edited by D. Capone et al., Elsevier, New York, 2005). In contrast, along the denser $\sigma = 27.5$ surface, the highest nitrate concentration are within the southern mode and intermediate waters, reaching 32.5 μM in the South Atlantic (Figure 10c).

[43] The difference between the maxima in the PO_4^* and nitrate distributions suggests that biotic processes lead to the elevated nitrate concentrations for lighter surfaces in the tropical Atlantic. The preferential enhancement of the nutrient concentrations on the lighter σ surfaces is a consequence of the remineralization of the particulate fallout being concentrated over the upper few hundred meters of the water column.

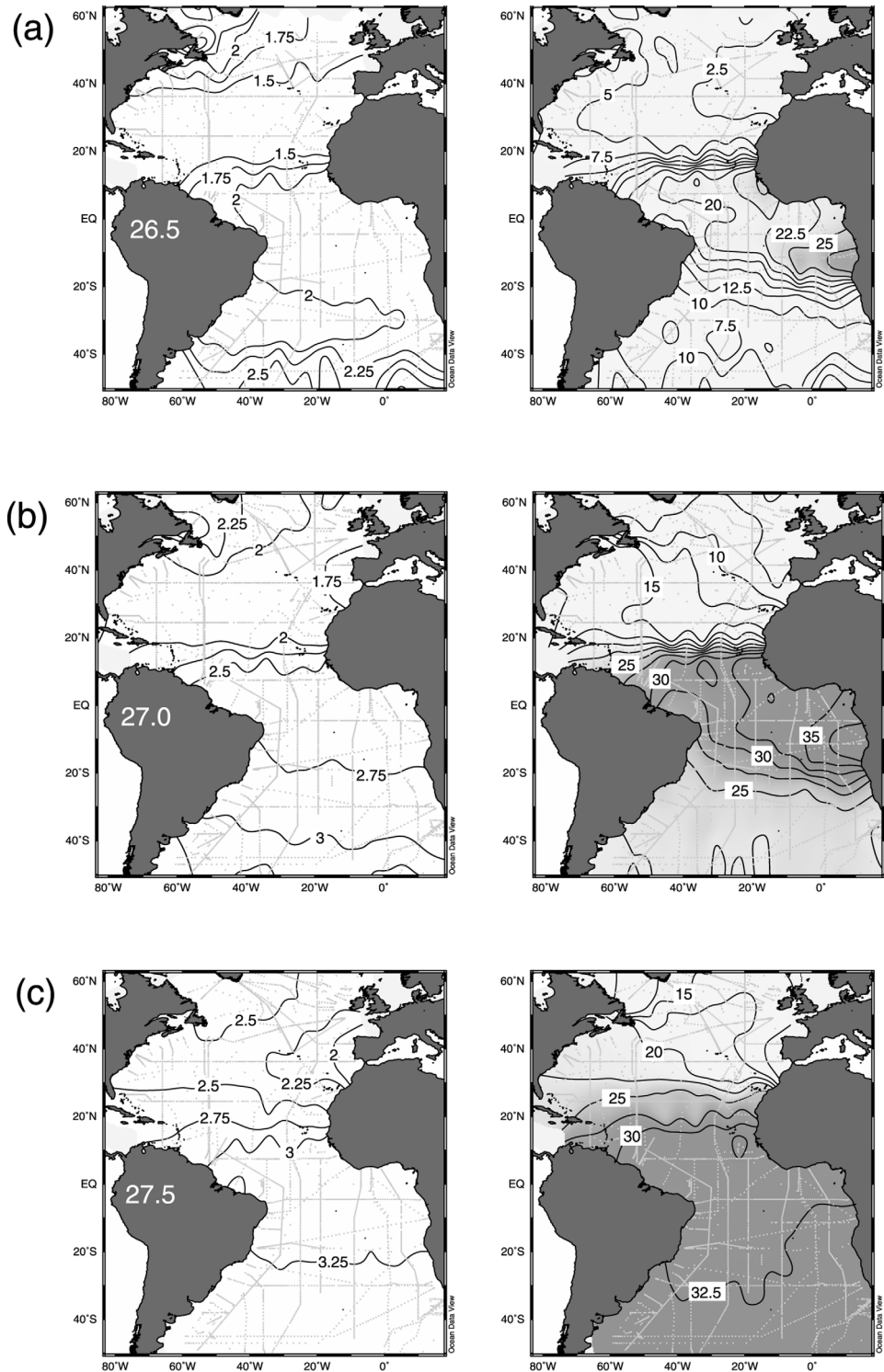


Figure 10. Diagnostics of (left) the conserved nutrient tracer, PO_4^* , and (right) nitrate in μM along (a) $\sigma = 26.5$, (b) $\sigma = 27.0$, and (c) $\sigma = 27.5$ surfaces for the Atlantic. Note how the PO_4^* tracer suggests a southern source, while the maximum nitrate concentrations are in the tropics for the lighter surfaces and in the South Atlantic for denser surfaces.

[44] In summary, the data diagnostics suggest that the ultimate nutrient source for the nutrient stream are the mode and intermediate waters from the Southern Ocean, as advocated by *Sarmiento et al.* [2004], together with a

weaker possible contribution from high-latitude subpolar waters. However, biotic processes play an important role in locally enhancing the nutrient concentrations in the tropics [*Toggweiler and Carson, 1995*]. Along the lighter

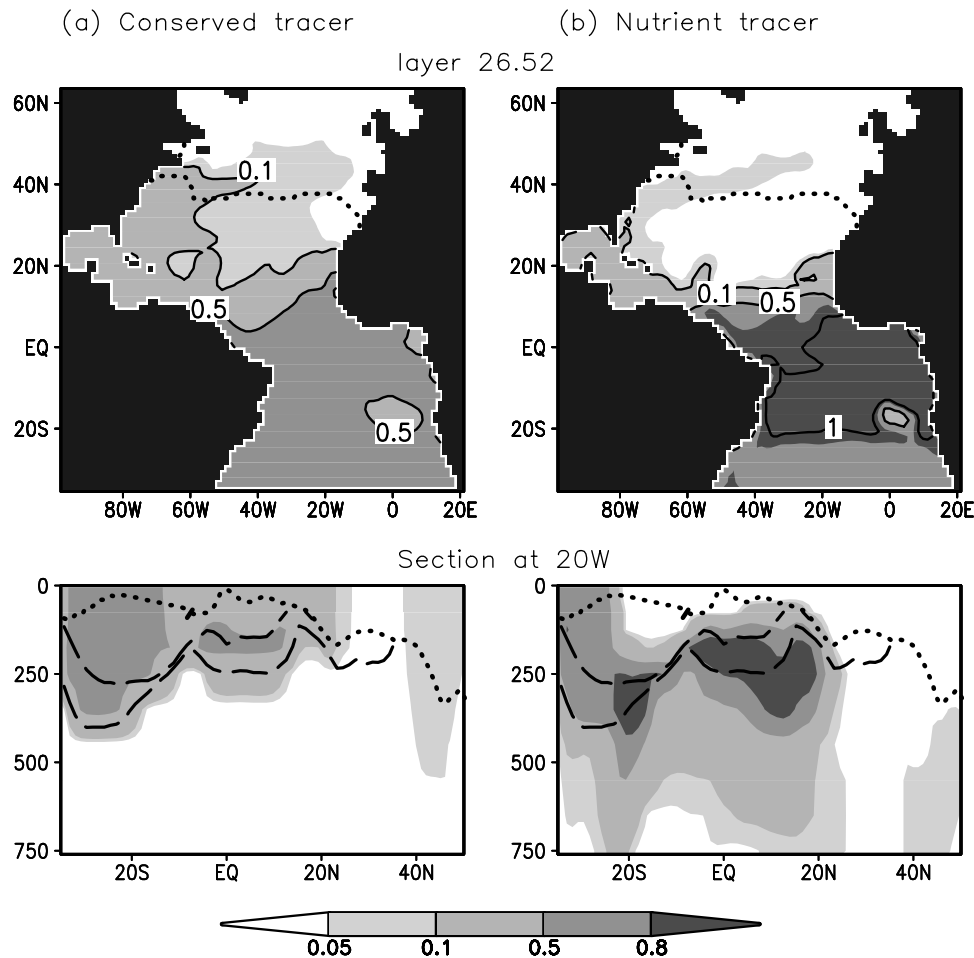


Figure 11. Twin experiments for tracer spreading from the South Atlantic (as in Figure 9) with the tracer either (a) conserved or (b) behaving like nitrate with consumption within the euphotic zone and remineralization at depth. Both tracer experiments are initialized with the same initial tracer distribution given by how a conserved tracer spreads for 20 years along $\sigma = 26.52$ with a continuous source of 1 in the South Atlantic at 20°S . The twin experiments are then integrated for a further 20 years without a source and with the tracer either (Figure 11a) conserved or (Figure 11b) behaving like nitrate. Note how the conserved tracer spreads farther over the northern subtropical gyre, but the nutrient tracer becomes concentrated at depth and has elevated concentrations in the tropics.

σ surfaces, this biotic cycling appears to be sufficiently strong to focus the nutrients onto these surfaces.

4.2.2. Model Tracer Experiments

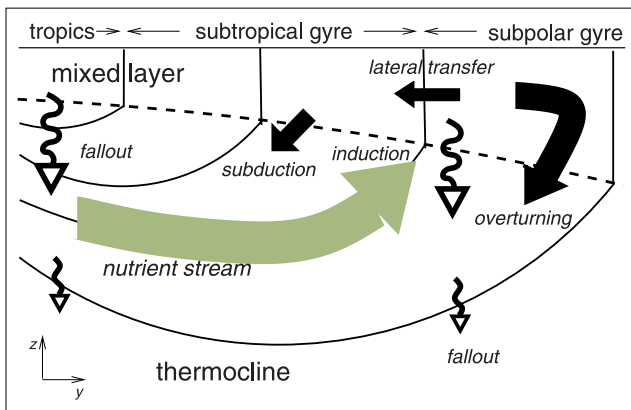
[45] The origins of the nutrient stream are now explored again using twin tracer experiments (as applied for the Gulf Stream). A tracer is continuously released with a value of 1 for 20 years within the model layer $\sigma = 26.52$ in a zonal band (four grid points wide) centered at 20°S across the South Atlantic. The patch of tracer is then tracked for a further 20 years integration, but with the tracer source switched off. The tracer is either treated as conserved or as a tracer mimicking the cycling of nitrate. Again, in both cases, the same volume of tracer is released in each experiment.

[46] First, for the conserved tracer, there is the expected northward spreading of the tracer away from the southern source (Figure 11a). After the total of 40 years integration, the patch of tracer is relatively uniform over the South

Atlantic within the source layer and there is a plume of tracer spreading northward along the western side of the northern subtropical gyre. At this stage of the integration, the tracer is concentrated in the mixed layer and the upper thermocline. The tracer spreads from the source into the lighter layers through diabatic transfer within the mixed layer, moving into a different density class, and then being subducted into the thermocline.

[47] Second, for the tracer mimicking nitrate, there is very little tracer within the winter mixed layer, apart from close to the original source region in the South Atlantic and a plume associated with the Gulf Stream along the western side of the northern subtropical gyre (Figure 11b). Instead, the tracer concentrations are elevated within the source layer and the upper thermocline at a depth of typically 250 m. There are particularly high tracer concentrations over the upwelling region of the tropics, comparable to the original tracer source prior to any dilution. This tropical signal is due

a) meridional view for a northern subtropical gyre



b) plan view of nutrient pathways

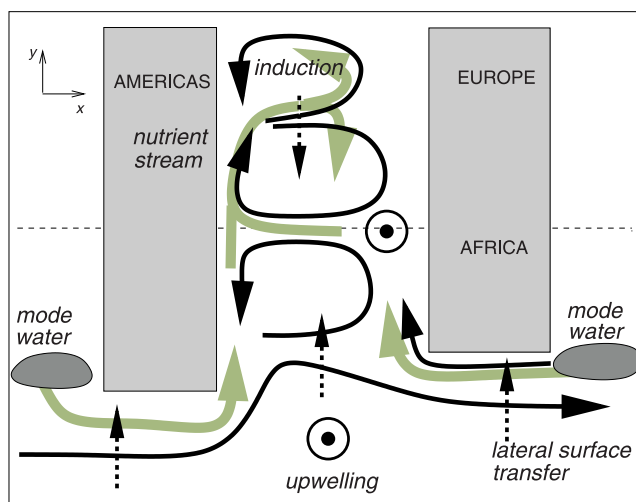


Figure 12. Schematic figure depicting (a) transfers within a subtropical gyre where the nutrient stream sustains the induction of nutrients into the mixed layer and (b) possible nutrient pathways in the Atlantic. Sub-Antarctic mode waters (gray shaded) are formed in the Southern Hemisphere, transferred northward, and eventually subducted, through the lateral Ekman (dashed line), gyre (black), and intermediate (gray) circulations. Nutrient concentrations are significantly enhanced in the tropics through the local vertical cycle of upwelling, fallout, and remineralization. This nutrient-rich water is then transferred into the northern basin through a nutrient stream associated with the boundary current.

to the vertical cycling of the nitrate tracer, where the tracer spends longer in the tropical upwelling zone and acquires higher concentrations from the remineralization of particle fallout; this process is often referred to as “nutrient trapping” [Najjar *et al.*, 1992]. Hence a maximum in the conserved tracer distribution reflect the expected spreading from a source, while maxima in the nitrate tracer distribution also reflect the effect of tropical upwelling locally concentrating the tracer. This “nutrient trapping” process is less pronounced when the tracer source is released into

denser model layers owing to the reduced interaction of the source layer with the euphotic zone

[48] Thus our interpretation of the isopycnal nitrate distributions in the data (Figure 10) is as follows: (1) The tropical enhancement along $\sigma = 26.5$ results from the recycling of fallout due to the nitrate influx into the euphotic zone from that layer; (2) the tropical enhancement along $\sigma = 27.0$ is instead a consequence of recycling of fallout from the euphotic zone stimulated by a nitrate influx from lighter layers; and (3) the lack of any tropical enhancement of nitrate along $\sigma = 27.5$ is due to this layer being too deep to experience significant remineralization. Thus the nitrate maxima along the σ surfaces are either located in the tropics where significant remineralization occurs or instead originate from the Southern Ocean mode waters.

5. Discussion

[49] Export production over the basin scale requires a nutrient supply to the euphotic zone to offset the loss of nutrients from organic fallout. Over a seasonal timescale, convection can often provide much of this necessary flux. However, convection only redistributes nutrients within the seasonal boundary layer. Again, if there is particulate fallout from this seasonal boundary layer, then there has to be a compensating influx of nutrients to sustain the patterns of export production.

[50] Over much of the basin circulation, this advective supply of nutrients is achieved through a combination of the nutrient streams, subsurface regions of high nitrate flux, and their subsequent, downstream transfer into the seasonal boundary layer (Figure 12a). The nutrient streams provide an influx of nutrients into both the subtropical and subpolar gyres, as first illustrated by *Pelegri and Csanady* [1991]. The subsequent advective transfer of nutrients into the seasonal boundary layer is provided by the induction process, the reverse of the subduction process that determines the interior water mass distributions. Our climatological diagnostics suggest that the induction of nutrients into the seasonal boundary layer is achieved by an isopycnal transfer into the winter mixed layer. This nutrient transfer is particularly strong following a cyclonic circuit of the subpolar gyre from the Gulf Stream to the Labrador Sea where the winter mixed layer becomes progressively denser and thicker downstream. Over the core of the nutrient stream, typically 40% of the nutrient flux associated with the boundary current at 36°N is transferred into the downstream winter mixed layer, while the remainder is probably recirculated. This advective input of nutrients acts to sustain the patterns of export production over the subpolar gyre. In regions where macro nutrients are not limiting, then the nutrients might ultimately be subducted through subpolar mode water formation or returned southward as part of the overturning circulation (Figure 12a).

[51] Over the oligotrophic subtropical gyres, the large-scale circulation only provides a nutrient influx into the mixed layer close to the Gulf Stream recirculation. More generally, fluid is subducted from the mixed layer into the underlying thermocline, as reflected in low nutrient concentrations in 18°C mode water being transferred into the upper thermocline [Palter *et al.*, 2005]. This transfer leads

to the classical problem of how export production is sustained over the subtropical gyres. On the flanks of the gyres, there can still be a surface lateral transfer through a combination of the horizontal Ekman flow and eddy, down-gradient transfers [Williams and Follows, 1998]. In the central part of the gyre, export production might be sustained through a vertical transfer through diapycnic [Pelegri and Csanady, 1994; Jenkins and Doney, 2003] or eddy vertical transfer processes [McGillicuddy *et al.*, 1998]. Alternatively, nitrogen fixation might provide the necessary nitrogen [Gruber and Sarmiento, 1997], although the required phosphorus still needs to be supplied. Transport and supply of semilabile DON and DOP also provide additional contributions of available N and P [Rintoul and Wunsch, 1991; Mahaffey *et al.*, 2004].

[52] On the larger basin scale of the Atlantic, the nutrient pathways reflect an interplay of the nutrient sources in the mixed layer and the gyre and intermediate circulations (Figure 12b). For the Atlantic, there is an influx of nutrients from the Southern Ocean linked to the transport of sub-Antarctic mode water, as recently emphasized by Sarmiento *et al.* [2004]. The sub-Antarctic mode water is formed on the equatorward side of the polar front. The mode water is transferred into the South Atlantic, from both the Indian Ocean via the Agulhas Current [Rintoul, 2005; Drijfhout *et al.*, 2005] and from the southeast Pacific through the Drake Passage [McCartney, 1982; Hanawa and Talley, 2001]. The mode water is transported northward, and eventually subducted, by the gyre and intermediate circulations. In the tropics, upwelling of these southern waters leads to a further enhancement of the nitrate concentrations through remineralization of the particulate fallout. A combination of the nutrient-rich southern waters and the tropical waters are then advected northward through the gyre circulation along the western boundary of the northern subtropical gyre. This nutrient stream then sustains the induction flux of nutrients over the northern basin (Figures 12a and 12b).

[53] While the eddy and frontal circulations are important in locally enhancing export production, they play a less significant role for the basin-scale transport of nutrients. The eddies probably are more significant at gyre boundaries in providing a down-gradient diffusive transfer along density surfaces. However, in our view, the basin-scale patterns of export production are primarily controlled by the pathway of the nutrient streams reflecting the boundary currents and the induction process associated with the gyre circulation.

[54] Our view has emphasized a climatologically averaged picture. However, the subduction and induction process is very sensitive to the thickness of the winter mixed layer, which varies year on year according to the buoyancy loss to the atmosphere and the background stratification. Consequently, interannual and decadal variations in the induction process are to be expected. This temporal variability will then accordingly lead to changes in surface nutrient concentrations and, if the nutrients are limiting, variations in export production.

[55] While this study has focused on the transport of nitrate, the induction process and action of nutrient streams are just as relevant for other tracers, such as iron. However, whether the induction process provides an enriched or

depleted supply of tracer to the mixed layer depends on the particular tracer source and the biogeochemical processes acting on the tracer as it is transported along isopycnals.

Appendix A: Nitrate and DON Model

[56] The evolution of nitrate, semilabile DON and refractory DON are given by

$$\frac{\partial}{\partial t} + \text{NO}_3^- + \nabla \cdot (\mathbf{u}\text{NO}_3^-) = F_{\text{NO}_3} \quad (\text{A1})$$

$$\frac{\partial}{\partial t} (\text{DON}_s + \text{DON}_r) + \nabla \cdot (\mathbf{u}(\text{DON}_s + \text{DON}_r)) = F_{\text{DON}}, \quad (\text{A2})$$

where \mathbf{u} is the three-dimensional velocity field, DON_s and DON_r are the semilabile and refractory forms of dissolved organic nitrogen, and F represents the sources and sinks of NO_3^- and DON.

A1. Within the Euphotic Zone

[57] The nitrate source/sink is given in (A1) by

$$F_{\text{NO}_3} = -G + \beta_s \text{DON}_s + \beta_r \text{DON}_r, \quad (\text{A3})$$

representing a loss from consumption of nitrate and a supply from the conversion of DON. The consumption of nitrate is given by

$$G = \alpha \left(\frac{I}{I + I_o} \right) \left(\frac{\text{NO}_3^-}{\text{NO}_3^- + \text{NO}_3^-_o} \right),$$

where α is the maximum consumption rate, I is the intensity of radiation and $\text{NO}_3^-_o$ is the nitrate concentration within the euphotic zone; here $\alpha = 1 \times 10^{-6} \mu\text{M s}^{-1}$, $I_o = 10 \text{ W m}^{-2}$ and $\text{NO}_3^-_o = 1.5 \mu\text{M}$.

[58] This consumption of nitrate leads to the formation of organic matter with a fraction a_{PON} converted to sinking PON, while the remainder forms DON advected by the flow. The partitioning between PON and DON formation varies with the background nitrate concentrations: the fraction of PON formed, a_{PON} , is chosen to be 0.5 in a nitrate-rich environment ($\text{NO}_3^- > 5 \mu\text{M}$) and only 0.2 in a nitrate-poor environment. When DON is formed from consumption of nitrate, a fraction of 0.4 is assumed to form semilabile DON, while the remainder is assumed to form refractory DON.

[59] The DON source/sink in (A2) is given by

$$F_{\text{DON}} = (1 - a_{\text{PON}})G - \beta_s \text{DON}_s - \beta_r \text{DON}_r, \quad (\text{A4})$$

where there is formation from the consumption of nitrate, as well as a loss from the conversion of semi-labile and refractory DON, which are assumed to occur on timescales of $\beta_s^{-1} = 6$ months and $\beta_r^{-1} = 6$ to 12 years; the breakdown of DON_r is assumed to occur photochemically and varies with irradiance.

A2. Below the Euphotic Zone

[60] The PON fallout flux is assumed to exponentially decay with depth below the euphotic zone (assumed to have

a thickness $h_e = 100$ m) down to the top of the densest model interface,

$$F(z) = F(-h_e) \exp(\gamma(z + h_e)), \quad (\text{A5})$$

with a remineralization depth scale given by $\gamma^{-1} = 200$ m and the flux assumed to vanish at the seafloor, so that there is no loss term of nutrients within the water column. The downward particulate flux is defined by $F(-h_e) = a_{PON} \int_{z=-h_e}^{z=0} G(z) dz$ at the base of the euphotic zone. Within the interior, nitrate is formed from the remineralization of PON and from the conversion of semi-labile DON in (A1),

$$F_{NO_3} = \frac{\partial F}{\partial z} + \beta_s DON_s, \quad (\text{A6})$$

while the semilabile DON is assumed to decay in the interior, but the refractory DON to remain conserved, such that in (A2),

$$F_{DON} = -\beta_s DON_s. \quad (\text{A7})$$

[61] **Acknowledgments.** The study was supported by a UK NERC 36N Consortium grant (NER/O/S/2003/00625). We thank Jorge Sarmiento and an anonymous referee for constructive feedback.

References

- Bleck, R., and L. T. Smith (1990), A wind-driven isopycnic coordinate model of the North and Equatorial Atlantic Ocean: 1. Model development and supporting experiments, *J. Geophys. Res.*, *95*, 3273–3285.
- Broecker, W. S., and T.-H. Peng (1982), *Tracers in the Sea*, 690 pp., Lamont-Doherty Earth Observ., Palisades, N. Y.
- Conkright, M. E., S. Levitus, and T. P. Boyer (1994), *World Ocean Atlas 1994*, vol. 1, *Nutrients*, NOAA Atlas NESDIS 1, 150 pp., Natl. Oceanic and Atmos. Admin., Silver Spring, Md.
- Drijfhout, S. S., J. M. H. Donners, and W. P. M. de Ruijter (2005), The origin of Intermediate and Subpolar Mode Waters crossing the Atlantic equator in OCCAM, *Geophys. Res. Lett.*, *32*, L06602, doi:10.1029/2004GL021851.
- Glover, D. M., and P. G. Brewer (1988), Estimates of wintertime mixed layer nutrient concentrations in the North Atlantic, *Deep Sea Res.*, *35*, 1525–1546.
- Gruber, N., and J. L. Sarmiento (1997), Global patterns of marine nitrogen fixation and denitrification, *Global Biogeochem. Cycles*, *11*, 235–266.
- Hanawa, K., and L. D. Talley (2001), Mode waters, in *Ocean Circulation and Climate: Observing and Modelling of the Global Ocean*, edited by G. Siedler, J. Church, and J. Gould, pp. 373–386, Elsevier, New York.
- Hogg, N. G. (1992), On the transport of the Gulf Stream between Cape Hatteras and the Grand Banks, *Deep Sea Res.*, *39*, 1231–1246.
- Isemer, H. J., and L. Hasse (1987), *The Bunker Climate Atlas of the North Atlantic Ocean*, vol 2, 252 pp., Springer, New York.
- Jenkins, W. J., and S. C. Doney (2003), The subtropical nutrient spiral, *Global Biogeochem. Cycles*, *17*(4), 1110, doi:10.1029/2003GB002085.
- Levitus, S. (1982), *Climatological Atlas of the World Ocean*, NOAA Prof. Pap. 13, 173 pp., Natl. Oceanic and Atmos. Admin., Silver Spring, Md.
- Mahaffey, C., R. G. Williams, G. A. Wolff, and W. Anderson (2004), The physical supply of nutrients to phytoplankton in the Atlantic, *Global Biogeochem. Cycles*, *18*, GB1034, doi:10.1029/2003GB002129.
- Marshall, J. C., A. J. G. Nurser, and R. G. Williams (1993), Inferring the subduction rate and period over the North Atlantic, *J. Phys. Oceanogr.*, *23*, 1315–1329.
- McCartney, M. S. (1982), The subtropical circulation of mode waters, *J. Mar. Res.*, *40*(suppl.), 427–464.
- McGillicuddy, D. J., A. R. Robinson, D. A. Siegel, H. W. Jannasch, R. Johnson, T. Dickey, J. McNeil, A. F. Michaels, and A. H. Knap (1998), New evidence for the impact of mesoscale eddies on biogeochemical cycling in the Sargasso Sea, *Nature*, *394*, 263–266.
- Najjar, R. G., J. L. Sarmiento, and J. R. Toggweiler (1992), Downward transport and fate of organic matter in the ocean: Simulations with a general circulation model, *Global Biogeochem. Cycles*, *6*, 45–76.
- Palter, J. B., M. S. Lozier, and R. T. Barber (2005), The impact of advection on the nutrient reservoir in the North Atlantic subtropical gyre, *Nature*, *437*, 687–692, doi:10.1038/nature03969.
- Pelegri, J. L., and G. T. Csanady (1991), Nutrient transport and mixing in the Gulf Stream, *J. Geophys. Res.*, *96*, 2577–2583.
- Pelegri, J. L., and G. T. Csanady (1994), Diapycnal mixing in western boundary currents, *J. Geophys. Res.*, *99*, 18,275–18,304.
- Pelegri, J. L., G. T. Csanady, and A. Martins (1996), The North Atlantic Nutrient Stream, *J. Oceanogr.*, *52*, 275–299.
- Pelegri, J. L., A. Marrero-Diaz, and A. W. Ratsimandresy (2006), Nutrient irrigation in the North Atlantic, *Prog. Oceanogr.*, in press.
- Qiu, B., and R. X. Huang (1995), Ventilation of the North Atlantic and North Pacific: Subduction versus obduction, *J. Phys. Oceanogr.*, *25*, 2374–2390.
- Rintoul, S. (2005), Nutrient return by the Southern Ocean overturning circulation: Efficacy, pathways and sensitivity to change, paper presented at Summer Meeting, Am. Soc. of Limnol. and Oceanogr., Santiago de Compostela, Spain.
- Rintoul, S. R., and C. Wunsch (1991), Mass, heat, oxygen and nutrient fluxes and budgets in the North Atlantic Ocean, *Deep Sea Res., Part I*, *38*, S355–S377.
- Roussenov, V., R. G. Williams, M. J. Follows, and R. M. Key (2004), The role of bottom water transport and diapycnic mixing in controlling the radiocarbon distribution in the deep Pacific, *J. Geophys. Res.*, *109*, C06015, doi:10.1029/2003JC002188.
- Sarmiento, J. L., N. Gruber, M. A. Brzezinski, and J. P. Dunne (2004), High-latitude controls of thermocline nutrients and low latitude biological productivity, *Nature*, *427*, 56–60.
- Toggweiler, J. R., and S. Carson (1995), What are upwelling systems contributing to the ocean's carbon and nutrient budgets?, in *Upwelling in the Ocean: Modern Processes and Ancient Records*, pp. 337–360, John Wiley, Hoboken, N. J.
- Usbeck, R., R. Schlitzer, G. Fisher, and G. Wefer (2003), Particle fluxes in the ocean: Comparison of sediment trap data with results from inverse modelling, *J. Mar. Syst.*, *39*, 167–183.
- Valdivieso da Costa, M., H. Mercier, and A. M. Treguier (2005), Effects of the mixed layer time variability on kinematic subduction rate diagnostics, *J. Phys. Oceanogr.*, *35*, 427–443.
- Williams, R. G. (2001), Ocean subduction, in *Encyclopedia of Ocean Sciences*, edited by J. H. Steele, K. K. Turekian, and S. A. Thorpe, pp. 1982–1993, Elsevier, New York.
- Williams, R. G., and M. J. Follows (1998), The Ekman transfer of nutrients and maintenance of new production over the North Atlantic, *Deep Sea Res., Part I*, *45*, 461–489.
- Williams, R. G., and M. J. Follows (2003), Physical transport of nutrients and the maintenance of biological production, in *Ocean Biogeochemistry: The Role of the Ocean Carbon Cycle in Global Change*, edited by M. Fasham, pp. 19–51, Springer, New York.
- Williams, R. G., A. McLaren, and M. J. Follows (2000), Estimating the convective supply of nitrate and implied variability in export production, *Global Biogeochem. Cycles*, *14*, 1299–1313.

M. J. Follows, Program in Atmospheres, Oceans and Climate, Department of Earth Atmosphere and Planetary Sciences, Massachusetts Institute of Technology, Cambridge, MA 02139, USA.

V. Roussenov and R. G. Williams, Department of Earth and Ocean Sciences, University of Liverpool, Liverpool L69 3GP, UK. (ric@liverpool.ac.uk)